Electronic absorption spectra and energy gap studies of Er^{3+} ions in different chlorophosphate glasses

Y.C. Ratnakaram [a,*], A. Viswanadha Reddy [a], R.P. Sreekanth Chakradhar [b]

[a] *Department of Physics, P.G. Centre, Sri Venkateswara University, Kavali 524 201, A.P., India*
[b] *Department of Physics, Indian Institute of Science, Bangalore 560 012, India*

Abstract

Spectroscopic properties of Er^{3+} ions in different chlorophosphate glasses $50P_2O_5$–$30Na_2HPO_4$–19.8RCl (R = Li, Na, K, Ca and Pb) are studied. The direct and indirect optical band gaps (E_{opt}) and the various spectroscopic parameters (E^1, E^2, E^3, and ξ_{4f} and α) are reported. The oscillator strengths of the transitions in the absorption spectrum are parameterized in terms of three Judd–Ofelt intensity parameters (Ω_2, Ω_4 and Ω_6). These intensity parameters are used to predict the transition probabilities (A), radiative lifetimes (τ_R), branching ratios (β) and integrated cross sections (Σ) for stimulated emission. Attention has been paid to the trend of the intensity parameters over hypersensitive transitions and optical band gaps. The lifetimes and branching ratios of certain transitions are compared with other glass matrices.

Keywords: Absorption spectra; Energy gap; Judd–Ofelt parameter; Radiative lifetime and branching ratio

1. Introduction

Solid state lasers have been employed in a wide variety of industrial and other applications. Glasses are attractive material for these applications, as they can be cast in large and optically homogeneous pieces. The spectroscopic properties and possible laser action in phosphate glasses have been a subject of many studies [1–4]. Erbium doped glasses are especially attractive for numerous applications such as eye-safe laser media [5] and as fiber amplifiers in long range telecommunications [6–8]. The first Er^{3+} doped glass laser utilizing the $^4I_{13/2} \rightarrow {}^4I_{15/2}$ transition at 1.5 μm was demonstrated by Snitzer and Wood Cock in a silicate glass [9]. The demonstration of the laser at this wavelength attracted attention since it is located in the 'eye safe' spectral region and could be detected easily [10–12]. Optical transitions and frequency up conversion emission of Er^{3+} ions in Ga_2S_3–GeS_2–La_2S_3 glasses were studied by Higuchi et al. [13]. Broad band excitation mechanism for photoluminescence in Er^{3+}-doped $Ge_{25}Ga_{1.7}As_{8.3}S_{65}$ glasses has been very well explained by Turnbull et al. [14]. Shojiya et al. [15] have given optical transitions of Er^{3+} ions in $ZnCl_2$ based glass.

* Corresponding author. Tel.: +91-8626-43858; fax: +91-8626-41847.

Binnemans and his co-researchers have given the spectroscopic properties of Er^{3+} ions in fluorophosphate glasses [16,17]. Tanabe et al. [18] studied Er^{3+} doped bismuth based boro-silicate glasses for their potential wavelength-division-multiplexing (WDM) amplifier. Recently Xian Feng et al. [19,20] reported the spectroscopic properties of Er^{3+} doped ultra-phosphate and germanotellurite glasses. Previously spectral investigations of Er^{3+} ions in sulphate [21] and chloroborate glasses [22] have been reported from our laboratories. Since the phosphate glasses have been the subject of several spectroscopic investigations, the authors took up the present investigation of the optical properties of Er^{3+} in different chlorophosphate glasses.

In this paper, the authors report the optical band gaps (E_{opt}) for indirect and direct transitions of different Er^{3+} doped chlorophosphate glasses. Spectral intensities (f) and intensity parameters (Ω_λ) for all the glasses studied have been reported. Radiative lifetimes (τ_R), branching ratios (β) and integrated cross sections (Σ) for stimulated emission for certain excited states $^4G_{11/2}$, $^4F_{5/2}$, $^4F_{7/2}$, $^4S_{3/2}$, $^4F_{9/2}$, $^4I_{9/2}$, $^4I_{11/2}$, and $^4I_{13/2}$ of Er^{3+} have been estimated and are presented in this paper. These spectral studies have been compared with other glass matrices and some of the potential lasing transitions have been identified.

2. Experimental

Different chlorophosphate glasses were prepared using a quenching technique from analar grades of P_2O_5, Na_2HPO_4, $ErCl_3$, LiCl, NaCl, KCl, $CaCl_2$ and $PbCl_2$. The general composition of the glasses was $50P_2O_5$–$30Na_2HPO_4$–19.8RCl (R = Li, Na, K, Ca and Pb) and 0.2 $ErCl_3$. The incorporation of the alkali contents reduced crystallization phenomena and increased stability of the glass. All these chemicals were obtained from different standard companies with 99.9% purity. The anhydrous chlorides were dried by heating at appropriate temperatures under vacuum. A small amount of ammonium chloride were added to these dehydrated chlorides in order to drive off impurities. About 5–10 g of batch composition was mixed in a specially made clay crucible and heated in an electric furnace for about 2 h at a temperature of 400 °C; this allowed the phosphorous pentoxide to decompose and react with other batch constituents before melting. The glass melting temperature was 1100–1150 °C and the melt was quenched in between two well polished brass disks. In order to obtain bubble free glass and to ensure homogeneity, the liquids were shaken at 15 min. interval during melting. Glass liquid was bubbled with oxygen to remove hydroxyl impurities. The prepared glass samples are transparent

Table 1
Certain physical properties of Er^{3+} doped chlorophosphate glasses

S. No.	Physical property	LiCPG	NaCPG	KCPG	CaCPG	PbCPG
1.	Average molecular Weight, M (g)	123.0	126.1	129.3	136.5	169.6
2.	Density, d (g/cm^3)	2.37	2.66	2.30	2.39	3.32
3.	Refractive index, n_d	1.495	1.489	1.492	1.483	1.510
4.	Molar refractivity, R_M (cm^{-3})	15.119	13.698	16.316	16.325	15.264
5.	Mean atomic volume, V (g/cm^3 per atom)	8.2	7.5	8.9	8.8	7.8
6.	Dielectric constant, ϵ	2.235	2.217	2.226	2.199	2.280
7.	Electronic polarizability, $\alpha_e \times 10^{24}$ (cm^3)	5.99	5.42	6.46	6.46	6.05
8.	Concentration, $N \times 10^{-22}$ (ions per cm^3)	0.232	0.253	0.214	0.211	0.236
9.	Ionic radius, r_i (Å)	3.042	2.954	3.126	3.143	3.026
10.	Inter-ionic distance r_p (Å)	7.549	7.331	7.757	7.799	7.509
11.	Field strength $F \times 10^{-16}$ (cm^2)	0.324	0.344	0.307	0.304	0.327
12.	Reflection losses, R (%)	3.936	3.859	3.897	3.784	4.128
13.	Ion packing ratio, V_P	20.917	18.774	22.366	22.378	20.913

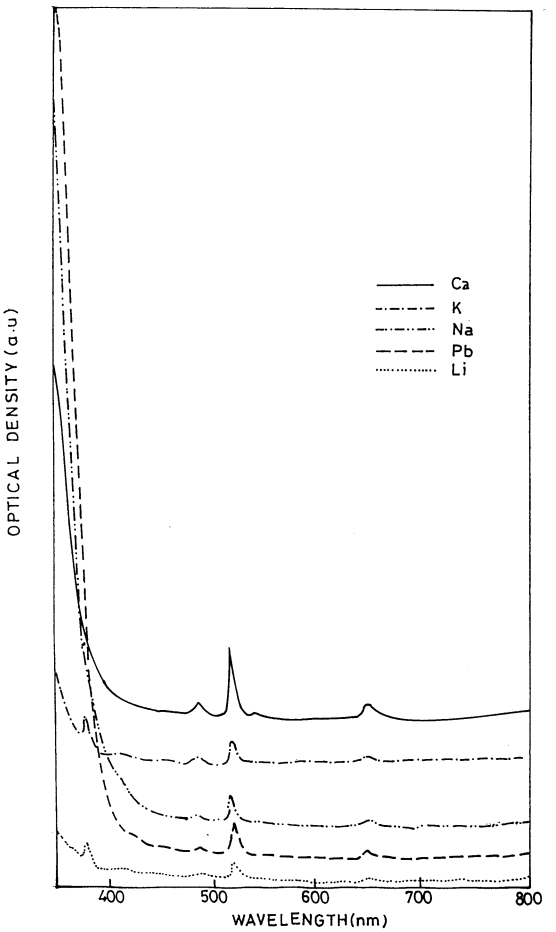

Fig. 1. Optical absorption edges of Er^{3+} doped different chlorophosphate glasses.

and 1–1.5 mm in thickness and circular in shape with 1 cm diameter. Density of the glass samples was determined by Archemede's principle using xylene as the immersion liquid with an accuracy of ± 0.005 g/cm^3. The glass refractive indices were measured using Abbe refractometer with an accuracy of ± 0.001. The absorption spectra were recorded in UV–VIS–NIR region using HITACHI U-3400 double beam spectrophotometer. Using these parameters, certain physical properties have been calculated by taking standard mathematical expressions [23–25].

The glass compositions are the formal glass composition $50P_2O_5$–$30Na_2HPO_4$–19.8 RCl (R = Li, Na, K, Ca and Pb)–$0.2ErCl_3$, although for the calculation of the various parameters, the actual composition was taken into account. The actual composition was calculated from the exact masses of the components in glass batch. There appears to negligible weight loss during melting (0.005 g in a 5 g batch) as seen by weighing the initial reaction mixture and the final product after melting and cooling. The symbols used in the tables and graphs in this article for the above glasses are LiCPG for lithium chlorophosphate glass, NaCPG for sodium chlorophosphate glass, KCPG for potassium chlorophosphate glass, CaCPG for calcium chlorophosphate glass and PbCPG for lead chlorophosphate glass.

3. Theory

Using Davis and Mott [26] theory, the optical data are analyzed for higher values of $\alpha(\omega)$ above the exponential region by plotting $(\alpha\hbar\omega)^{1/2}$ as a function of photon energy $\hbar\omega$ for indirect transitions and by plotting $(\alpha\hbar\omega)^2$ as a function of $\hbar\omega$ for direct transitions. The optical band gaps 'E_{opt}' values are obtained by extrapolation to $(\alpha\hbar\omega)^{1/2} = 0$ and $(\alpha\hbar\omega)^2 = 0$ for indirect and direct transitions, respectively. The values of 'E_g' which are interpreted as the width of the tail of localized states in the forbidden band gap are estimated from the plots of $\ln \alpha$ versus $\hbar\omega$.

The energy E_J of the Jth level may be written in terms of the changes in the parameters by a Tayler's series expansion [27,28] as:

$$E_J = E_{0J} + \sum_{k=1}^{3} \frac{dE_J}{dE^k}\Delta E^k + \frac{dE_J}{d\xi}\Delta\xi_{4f} + \frac{dE_J}{d\alpha}\Delta\alpha + \ldots\ldots \quad (1)$$

where E_{0J} is the zero order energy of the J^{th} level and dE_J/dE^k, $dE_J/d\xi$ and $dE_J/d\alpha$ are partial derivatives. The partial derivatives have been evaluated using aquo ion parameters using the method of Wong [27,28]. Using experimental energies as E_J and the numerical values of zero order energies and partial derivatives, a number of linear equations equal to the number of observed levels are formed and the delta values are calculated by using the least-squares fit method. The E^k, ξ_{4f} and α parameters are evaluated from:

$$E^k = E^{0k} + \Delta E^k \tag{2}$$

$$\xi_{4f} = \xi^0 + \Delta\alpha \tag{3}$$

$$\alpha = \alpha^0 + \Delta\alpha \tag{4}$$

where E^{0k}, ξ^0, α^0 are the aqua ion parameters with which the partial derivatives were evaluated. Using these Δ and E_{0J} values and partial derivatives the energy values E_J have been calculated. To measure the quality of the fit between experimental and calculated values, the rms deviation has been calculated using the formula:

$$\delta_{\text{rms}} = \sqrt{\frac{\Delta^2}{M-N}} \tag{5}$$

where Δ^2 is the sum of the squares of the deviation, M is the number of levels used for fitting and N is the number of parameters.

The intensities of the absorption bands are determined using the area method and using the formula:

$$f_{\text{exp}} = 4.32 \times 10^{-9} \int \epsilon(v)\mathrm{d}v \tag{6}$$

where $\epsilon(v)$ is the molar extinction coefficient corresponding to the energy of the transition v. According to Judd–Ofelt theory [30,29]:

$$f_{\text{ed}} = \sum_{\lambda=2,4,6} T_\lambda v(f^N\psi J\|U^\lambda\|f^N\psi' J')^2 \tag{7}$$

the three parameters T_2, T_4 and T_6 are evaluated using the experimental data employing least-squares fit. The squared reduced matrix elements $\|U^\lambda\|^2$ in the above equation are calculated in the intermediate coupling case. As these values are insensitive to the environment, we have used the values given by Carnall et al. [31]. With these T_2, T_4 and T_6 parameters and squared reduced matrix elements, 'f_{cal}' values are evaluated.

The Judd–Ofelt intensity parameters (Ω_λ) are calculated from the formula:

$$\Omega_\lambda(\text{cm}^2) = \left(\frac{3h}{8\pi^2 mc}\right)\left(\frac{9n}{(n^2+2)^2}\right)(2\mathrm{J}+1)T_\lambda \tag{8}$$

where n is the refractive index of the glass.

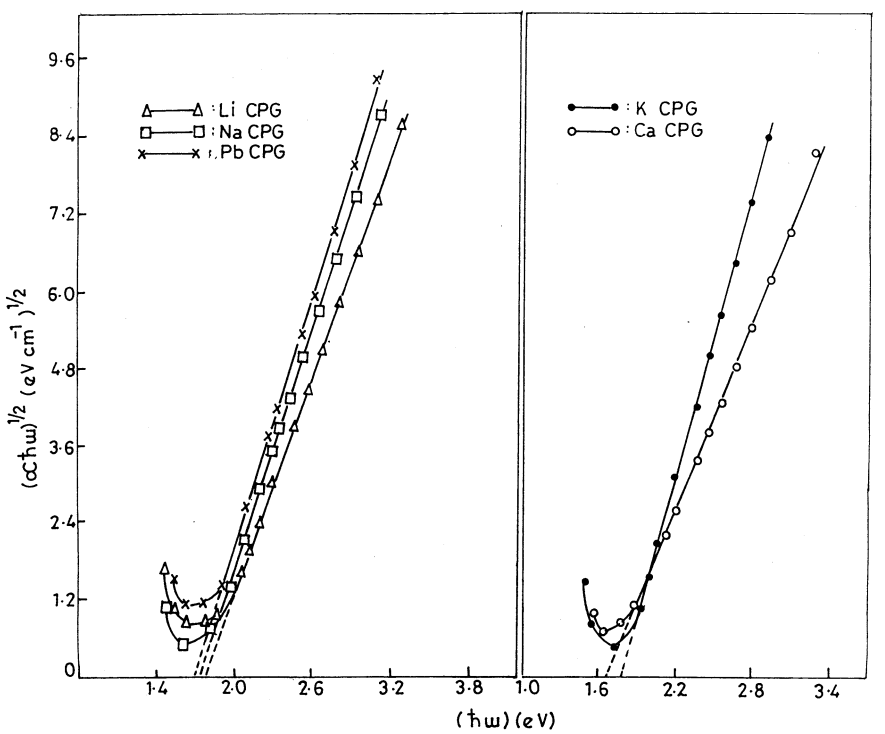

Fig. 2. The relation between $(\alpha\hbar\omega)^{1/2}$ and $\hbar\omega$ for different Er^{3+} doped chlorophosphate glasses.

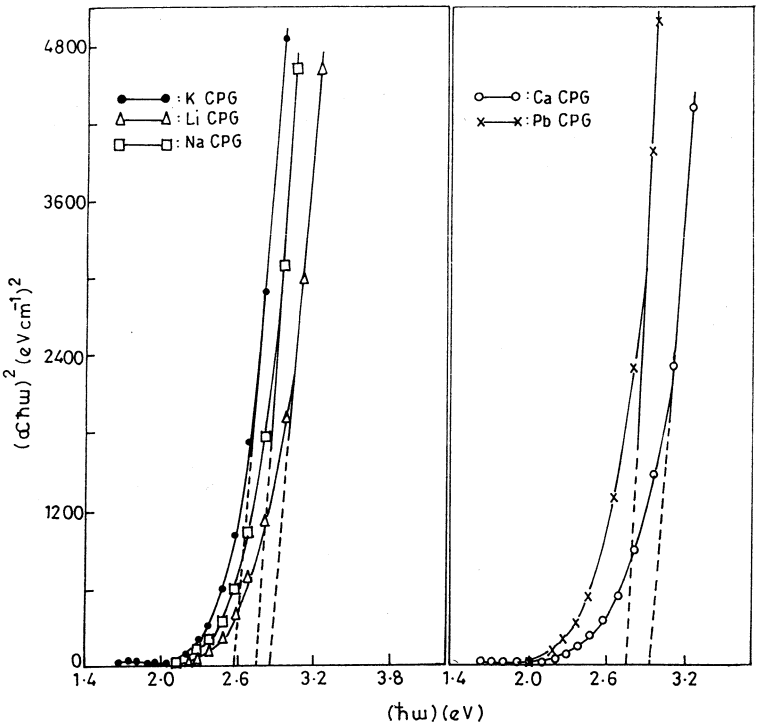

Fig. 3. The relation between $(\alpha\hbar\omega)^2$ and $\hbar\omega$ for different Er^{3+} doped chlorophosphate glasses.

Table 2
Some of the optical measurements of Er^{3+} doped chlorophosphate glasses

S. No.	Glass	Average molecular weight (g)	E_{opt} (eV)		E_g (eV)	B (cm eV)$^{-1}$	B (cm^{-1} eV$^{1/2}$)
			Indirect transitions	Direct transitions		Indirect transitions	Direct transitions
1.	LiCPG	123.0	1.79	2.86	0.48	32.1	121.3
2.	NaCPG	126.1	1.77	2.76	0.55	40.7	134.7
3.	KCPG	129.3	1.76	2.59	0.50	50.7	120.7
4.	CaCPG	136.5	1.65	2.95	0.58	31.0	112.4
5.	PbCPG	169.6	1.67	2.80	0.53	36.9	111.8

The electric dipole line strengths are calculated employing the formula:

$$S_{ed} = e^2 \sum_{\lambda = 2,4,6} \Omega_\lambda (\psi J \| U^\lambda \| \psi' J')^2 \tag{9}$$

The radiative transition probability is given by:

$$A = \left(\frac{64\pi^4 v^3}{3h(2J+1)}\right)\left(\frac{n(n^2+2)^2}{9}\right) S_{ed} \tag{10}$$

and is related to the radiative lifetime τ_R, of an excited state by the expression:

$$\tau_R = A_T(\psi J)^{-1} \tag{11}$$

where $A_T(\psi J)$ is the total radiative transition probability. The radiative branching ratio is defined as:

$$\beta(\psi J, \psi' J') = \frac{A(\psi J, \psi' J')}{A_T(\psi J)} \tag{12}$$

The integrated absorption cross section (Σ) is evaluated from:

$$\sum = \frac{1}{v^2}\frac{A}{8\pi c n^2} \tag{13}$$

4. Results and discussion

4.1. Physical properties

Table 1 gives some of the physical properties of the Er^{3+} doped chlorophosphate glasses which are calculated from the densities, refractive indices and average molecular weights of the glasses. The ion packing ratio (V_P) which is the property of the glass host is calculated using the formula [32]:

$$V_P = \sum_i \frac{4}{3}\pi r_p^3 n_i \frac{N_A}{V_m} \tag{14}$$

where r_p is the ionic radius, n_i is the molar fraction, N_A is the Avagadro number and V_m is the molar volume. It is observed that the ion packing ratio decreases with the decrease of ionic radius in the order Ca > K > Li > Pb > Na as reported in literature [32]. Among all the glasses studied, sodium glass has the lowest ion packing ratio. It is also noticed that sodium chlorophosphate glass has the lowest molar refractivity, mean atomic volume, electronic polarizability, ionic radius, inter ionic distance and highest field strength.

4.2. Optical band gaps

Fig. 1 shows the absorption edges of different Er^{3+} doped chlorophosphate glasses. From the spectra, it can be seen that the position of the fundamental absorption edge shifts to longer wavelengths with an increase of average molecular weight of the glass. But for sodium chlorophosphate glass it was not followed. It may be due to

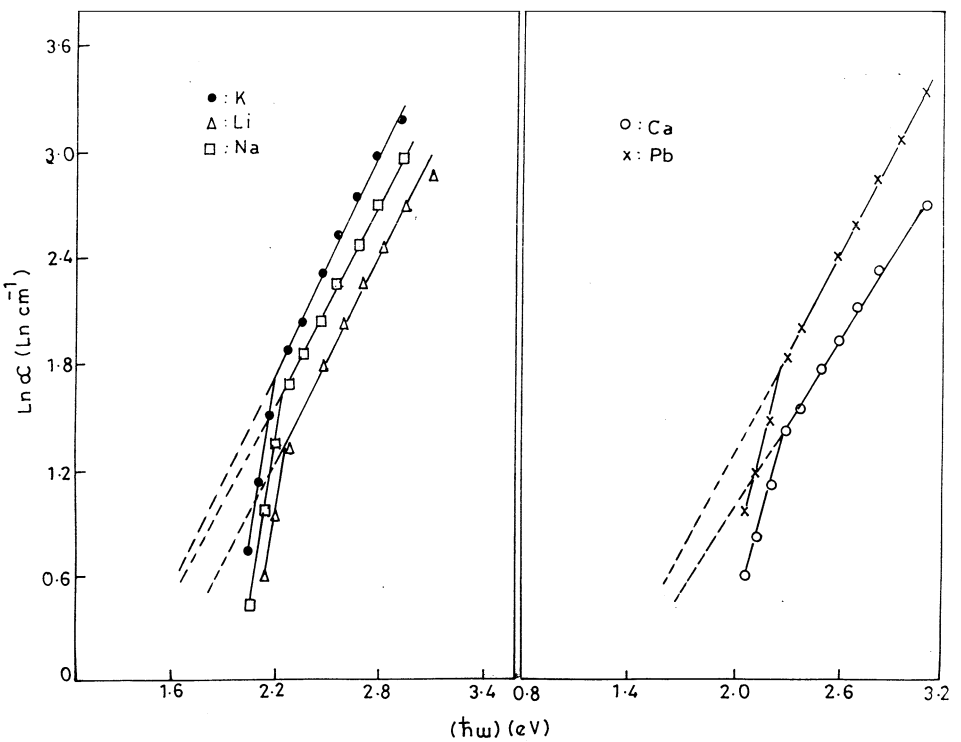

Fig. 4. The relation between ln α and $\hbar\omega$ for different Er^{3+} doped chlorophosphate glasses.

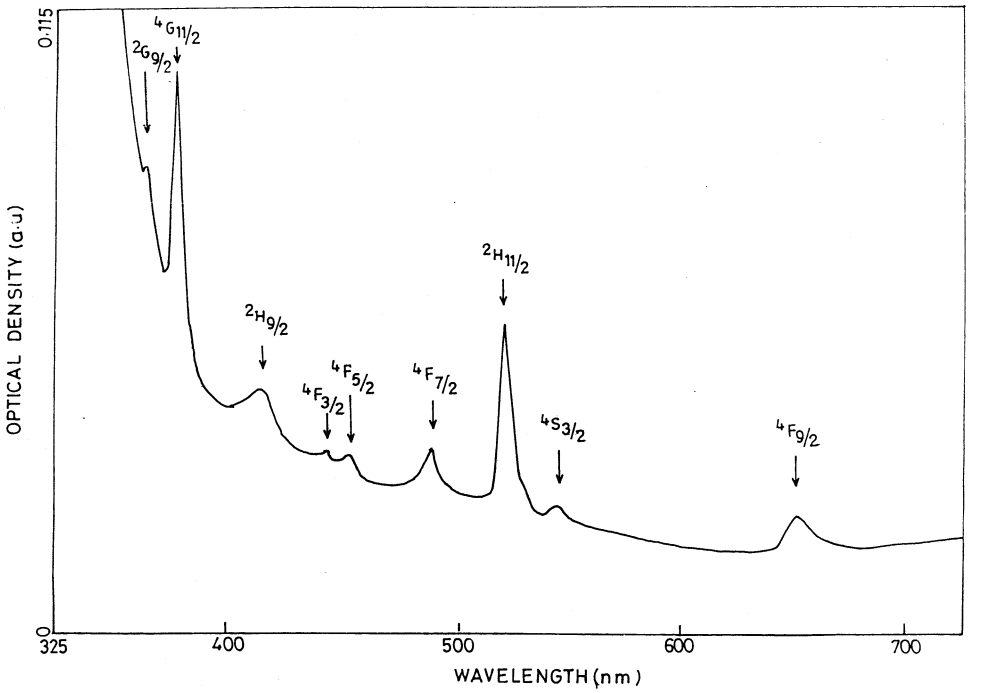

Fig. 5. Optical absorption spectrum of Er^{3+} doped lithium chlorophosphate glass.

Table 3
Energies, various spectroscopic parameters and hydrogenic ratios of Er^{3+} doped chlorophosphate glasses (all values except $E^1/E^3$and E^2/E^3 are in cm^{-1})

S. No.	Energy Level	LiCPG		NaCPG		KCPG		CaCPG		PbCPG	
		E_{expt}	E_{cal}	E_{expt}	E_{cal}	E_{expt}	E_{cal}	E_{expt}	E_{cal}	E_{expt}	E_{cal}
1.	$^4F_{9/2}$	15 382	15 238	15 359	15 333	15 366	15 282	15 359	15 258	15 366	15 304
2.	$^4S_{3/2}$	18 411	18 449	18 404	18 401	18 347	18 346	18 411	18 419	18 431	18 452
3.	$^2H_{11/2}$	19 236	19 203	19 235	19 241	19 236	19 241	19 236	19 208	19 236	19 244
4.	$^4F_{7/2}$	20 498	20 474	20 553	20 575	20 486	20 520	20 511	20 506	20 528	20 568
5.	$^4F_{5/2}$	22 093	22 062	22 049	22 045	22 216	22 186	22 093	22 103	22 191	22 189
6.	$^4F_{3/2}$	22 567	22 451	22 443	22 526	22 638	22 473	22 460	22 465	22 562	22 526
7.	$^2H_{9/2}$	24 533	24 514	24 533	24 809	24 557	24 565	24 533	24 501	24 569	24 536
8.	$^4G_{11/2}$	26 517	26 573	–	–	26 517	26 611	26 517	26 616	26 546	26 658
9.	$^2G_{9/2}$	27 517	27 605	–	–	27 670	27 744	–	–	–	–
	rms deviation	±111		±205		±111		±85		±83	
	E^1	6636		6556		6675		6632		6645	
	E^2	30.7		28.5		32.6		31.2		31.7	
	E^3	643		648		641		646		644	
	ξ_{4f}	2380		2408		2448		2395		2417	
	α	−1.72		1.26		1.88		0.63		0.07	
	E^1/E^3	10.32		10.11		10.40		10.26		10.31	
	E^2/E^3	0.048		0.044		0.051		0.048		0.049	

certain structural changes that may have occurred in the sodium chlorophosphate glass. Among these five Er^{3+} doped glasses, lithium and lead chlorophosphate glasses show the shortest and largest shift of the absorption edge. It is also clear that there is no sharp absorption edge and this is the characteristic of the glassy state just as the X-ray diffraction spectra also show a broad featureless curve.

Figs. 2 and 3 represent the variation of $(\alpha\hbar\omega)^{1/2}$ versus $\hbar\omega$ and $(\alpha\hbar\omega)^2$ versus $\hbar\omega$ for indirect and direct transitions, respectively. The optical band gap values 'E_{opt}' obtained by extrapolation to $(\alpha\hbar\omega^2 = 0$ and $(\alpha\hbar\omega)^2 = 0$ and the constant 'B' values are presented in Table 2 for all the glasses studied. From the table it is observed that lithium and calcium chlorophosphate glasses are having the highest and lowest 'E_{opt}' values for indirect transitions whereas for direct transitions potassium and calcium glasses are having the lowest and highest values. The 'E_{opt}' values decrease with the increase of average molecular weight of the glass for only alkali elements for both direct and indirect transitions. Fig. 4 represents the plots of $\ln \alpha$ and $\hbar\omega$. The 'E_g' values obtained from the plots are also presented in Table 2. There is no systematic variation in these values except the lowest 'E_g' value observed in lithium glass.

Table 4
Experimental and calculated oscillator strengths ($f \times 10^6$) of Er^{3+} doped different chlorophosphate glasses

S. No.	Energy level	LiCPG		NaCPG		KCPG		CaCPG		PbCPG	
		f_{expt}	f_{cal}	f_{expt}	f_{cal}	f_{expt}	f_{cal}	f_{expt}	f_{cal}	f_{expt}	f_{cal}
1.	$^4F_{9/2}$	2.362	2.275	2.343	2.333	1.947	2.026	3.890	3.981	6.360	6.341
2.	$^4S_{3/2}$	0.755	0.568	1.052	0.613	1.173	1.122	1.372	1.461	1.164	1.223
3.	$^2H_{11/2}$	7.185	8.019	3.704	3.692	13.503	11.705	21.609	19.855	28.597	25.454
4.	$^4F_{7/2}$	1.834	2.242	2.343	2.383	3.944	3.559	5.548	5.103	5.207	5.340
5.	$^4F_{5/2}$	1.499	0.681	0.377	0.733	0.517	1.356	0.982	1.750	1.996	1.470
6.	$^4F_{3/2}$	0.311	0.393	0.293	0.421	0.538	0.781	0.687	1.005	0.690	0.844
7.	$^2H_{9/2}$	5.496	—	—	—	7.994		2.462		1.955	—
8.	$^4G_{11/2}$	15.039	14.121	—	—	18.693	20.626	33.101	34.979	41.486	44.877
9.	$^2G_{9/2}$	1.422	0.921	—	—	—	—	—	—	—	—
10.	rms deviation	—	±0.73	—	±0.33	—	±1.40	—	±1.37	—	±2.33

Table 5
Judd–Ofelt intensity parameters (Ω_2, Ω_4, Ω_6; 10^{-20} cm^2) and intensities ($f \times 10^6$) of the hypersensitive transitions of Er^{3+} in different glass matrices

Glass	Ω_2	Ω_4	Ω_6	f ($^4I_{9/2} \rightarrow {}^2H_{11/2}$)	f ($^4I_{9/2} \rightarrow {}^2G_{11/2}$)
$50P_2O_5$–$30Na_2HPO_4$–19.8LiCl (present work)	2.965	0.948	0.864	7.185	15.039
$50P_2O_5$–$30Na_2HPO_4$–19.8NaCl (present work)	1.013	0.938	0.936	3.704	–
$50P_2O_5$–$30Na_2HPO_4$–19.8KCl (present work)	5.049	0.054	1.715	13.503	18.693
$50P_2O_5$–$30Na_2HPO_4$–19.8$CaCl_2$ (present work)	8.144	1.075	2.240	21.609	33.101
$50P_2O_5$–$30Na_2HPO_4$–19.8$PbC1_2$ (present work)	9.366	3.069	1.836	28.597	41.486
$80H_3BO_3$–$10Na_2CO_3$–10LiCl[22]	6.369	0.651	1.018	–	–
$80H_3BO_3$–$10Na_2CO_3$–10NaC1[22]	5.220	1.236	0.466	–	–
$80H_3BO_3$–$10Na_2CO_3$–10KC1[22]	6.116	0.198	1.377	–	–
$80H_3BO_3$–l0Na_2CO_3–l0$PbCl_2$[22]	4.536	1.589	0.382	–	–
$75NaPO_3$–$20CaF_2$–$5ErF_3$[16]	2.250	1.010	0.800	–	–
$30Li_2O$–$60P_2O_5$–$10A1_2O_3$[23]	6.420	1.640	0.780	–	–

Table 6
Electric dipole line strengths ($S_{ed}/e^2 \times 10^{22}$), transition probabilities (A), branching ratios (β) and integrated cross sections ($\Sigma(10^{-18})$ of Er^{3+} doped lithium chlorophosphate glass and branching ratios in $ZnCl_2$ [15] and $ZnBO_3$ [36] glasses

Transition		ν (cm^{-1})	S_{ed}/e^2 (cm^2)	A (s^{-1})	β	Σ (cm^{-1})	β [15]	β [36]
$^4G_{11/2} \rightarrow$	$^2H_{9/2}$	2059	137.7	2.1	0	0.299	–	–
	$^4F_{3/2}$	4122	10.0	1.2	0	0.043	–	–
	$^4F_{5/2}$	4511	10.5	1.7	0	0.050	–	–
	$^4F_{7/2}$	6099	39.1	15.9	0.001	0.253	–	–
	$^2H_{11/2}$	7370	18.7	13.4	0.001	0.146	0	–
	$^4S_{3/2}$	8125	12.9	12.0	0.001	0.108	0	–
	$^4F_{9/2}$	11 335	131.5	343.5	0.032	1.586	0.03	–
	$^4I_{9/2}$	14 244	21.8	113.2	0.010	0.331	0.01	–
	$^4I_{11/2}$	16 344	5.7	45.2	0.004	0.100	0.01	–
	$^4I_{13/2}$	20 061	77.0	1115.2	0.104	1.644	0.06	–
	$^4I_{15/2}$	26 573	269.3	9064.9	0.845	7.618	0.89	–
$^4F_{5/2} \rightarrow$	$^4F_{7/2}$	1588	36.0	0.5	0	0.122	–	–
	$^2H_{11/2}$	2859	21.4	1.8	0.001	0.129	–	–
	$^4S_{3/2}$	3614	2.6	0.4	0	0.019	–	–
	$^4F_{9/2}$	6824	52.5	59.8	0.039	0.762	–	–
	$^4I_{9/2}$	9733	18.6	61.7	0.040	0.386	–	–
	$^4I_{11/2}$	11 833	9.5	56.8	0.037	0.240	–	–
	$^4I_{13/2}$	15 550	46.5	627.3	0.406	1.539	–	–
	$^4I_{15/2}$	22 062	19.1	735.8	0.476	0.897	–	–
$^4F_{7/2} \rightarrow$	$^2H_{11/2}$	1271	73.2	0.4	0	0.147	–	–
	$^4S_{3/2}$	2026	0.5	0	0	0.001	–	–
	$^4F_{9/2}$	5236	8.0	3.1	0.001	0.066	–	–
	$^4I_{9/2}$	8145	50.8	73.9	0.037	0.661	–	–
	$^4I_{11/2}$	10 245	39.5	114.2	0.057	0.645	–	–
	$^4I_{13/2}$	13 962	32.2	235.8	0.118	0.717	–	–
	$^4I_{15/2}$	20 474	67.9	1569.5	0.786	2.222	–	–
$^4S_{3/2} \rightarrow$	$^4F_{9/2}$	3210	1.9	0.3	0	0.020	–	–
	$^4I_{9/2}$	6119	29.1	35.8	0.037	0.567	0.05	0.035
	$^4I_{11/2}$	8219	7.0	21.0	0.022	0.184	0.02	0.022
	$^4I_{13/2}$	11 936	29.2	267.2	0.277	1.113	0.28	0.276
	$^4I_{15/2}$	18 448	18.9	641.3	0.664	1.118	0.65	0.666
$^4F_{912} \rightarrow$	$^4I_{9/2}$	2909	38.5	2.0	0.009	0.143	0.01	0.004
	$^4I_{11/2}$	5009	20.2	5.5	0.025	0.129	0.04	0.052
	$^4I_{13/2}$	8725	62.2	89.0	0.412	0.693	0.06	0.046
	$^4I_{15/2}$	15 238	15.6	119.2	0.552	0.304	0.89	0.899
$^4I_{9/2} \rightarrow$	$^4I_{11/2}$	2100	20.3	0.4	0.004	0.054		0.010
	$^4I_{13/2}$	5817	62.0	26.3	0.293	0.461	–	0.033
	$^4I_{15/2}$	12 329	15.6	63.1	0.702	0.246		0.686
$^4I_{11/2} \rightarrow$	$^4I_{13/2}$	3717	120.3	11.1	0.120	0.476	0.08	0.147
	$^4I_{15/2}$	10 229	42.2	81.0	0.880	0.459	0.92	0.850
$^4I_{13/2} \rightarrow$	$^4I_{15/2}$	6512	140.6	59.7	1.000	0.835	1.00	1.000

4.3. Energy levels

The absorption spectrum of Er^{3+} doped lithium chlorophosphate glass is shown in Fig. 5. The remaining spectra are not shown as they are of similar shape. From the recorded spectra of all the glasses it is noticed one important feature i.e. the transition $^4I_{15/2} \rightarrow {}^4G_{11/2}$ of Er^{3+} is not observed only in sodium chlorophosphate glass, as the cut off region starts from 400 nm in this glass. The experimental and calculated energies (E_J) and various spectroscopic parameters (E^1, E^2, E^3, ξ_{4f} and α) obtained for all these Er^{3+} doped glasses are presented in Table 3. The energy values of the

levels $^4G_{11/2}$ and $^2G_{9/2}$ are not included in the above least square fitting calculations. From the table it is observed that the rms deviations between experimental and calculated energies are within experimental error. The radial properties of Er^{3+} ions remain unchanged as the hydrogenic ratios E^1/E^3 and E^2/E^3 are nearly constant for all the glasses. The spin-orbit coupling parameter ξ_{4f} increases with the increase of average molecular weight of the glass for only alkali elements.

4.4. Spectral intensities

The spectral intensities for different absorption bands of Er^{3+} doped chlorophosphate glasses are determined using Eqs. (6) and (7) given in the theoretical part. The experimental and calculated spectral intensities for all the transitions are presented in Table 4 for all the glasses. As there is some uncertainty in the measurement of the intensities of the bands $^2H_{9/2}$ and $^2G_{9/2}$, these intensities are not included in the least square fit in calculating the Judd–Ofelt intensity parameters for all the glasses. The agreement between the experimental and calculated spectral intensities is good which shows the validity of the approximations made in Judd–Ofelt theory. From the table, it can be discerned that the intensities of the transitions are high in lead chlorophosphate glass which indicates that the non-symmetric component of the electric field acting on the Er^{3+} ions is very strong in this glass.

The best set of intensity parameters (Ω_2, Ω_4 and Ω_6) is obtained from the experimental oscillator strengths and the doubly reduced matrix elements using the expression Eq. (8) and using least-square analysis. The Judd–Ofelt intensity parameters in all the chlorophosphate glasses along with the parameters in various glass matrices are presented in Table 5. The position and intensity of certain electric dipole transitions of rare earth ions are found to be very sensitive to the environment of the rare earth ion. Such transitions are called hypersensitive transitions. These transitions will obey certain selection rules. The intensities of these hypersensitive transitions i.e. $^4I_{9/2} \rightarrow {}^2H_{11/2}$ and $^4I_{9/2} \rightarrow {}^4G_{11/2}$ of Er^{3+} ion are also included in the above table. It is observed that the intensities of the hypersensitive transitions decrease with the decrease of Ω_2 parameter which is in accordance with the theory [33]. It indicates that there is a strong interaction between 4f and 5d orbitals. Jorgensen and Reisfeld [34] noted that the Ω_2 parameter is indicative of the amount of covalent bonding while the Ω_6 parameter is related to rigidity of the host. The Ω_2 parameter is larger in lead chlorophosphate glass and smaller in sodium chlorophosphate glass which shows low ionicity (high covalency) and high ionicity (low covalency) between erbium cation and chloride anion in these glasses correspondingly. It is also observed that except for sodium chlorophosphate glass, Ω_2 parameter is increasing with the increase of average molecular weight of the glass which indicates that the amount of covalency is increasing with the substitution of lithium, potassium, calcium and lead in these glasses.

It is also seen that Ω_4 parameter decreases and Ω_6 parameter increases with the increase of average molecular weight of the glass for only alkali elements (Li, Na and and K). By comparing these parameters with various glass matrices, it is observed that Ω_2 parameter is smaller in sodium

Table 7
Estimated radiative lifetimes (τ_R;(μs)) of certain excited states of Er^{3+} doped different chlorophosphate glasses

S. No.	Energy level	LiCPG	NaCPG	KCPG	CaCPG	PbCPG	BaF_2–ThF_2 [37]	$ZnBO_3$ [36]
1.	$^4G_{11/2}$	93	109	58	39	34	–	–
2.	$^4F_{5/2}$	647	627	411	289	262	–	–
3.	$^4F_{7/2}$	500	478	367	240	192	–	–
4.	$^4S_{3/2}$	1035	976	544	410	467	960	333
5.	$^4F_{9/2}$	4635	4524	5242	2647	1631	950	418
6.	$^4I_{9/2}$	11 135	10 776	18 409	7278	3796	8180	3554
7.	$^4I_{11/2}$	10 857	11 086	5522	4242	4428	10 200	3483
8.	$^4I_{13/2}$	16 750	15 698	8453	6766	6849	10 200	4378

Table 8
Branching ratios (β) and integrated cross sections (Σ; (10^{-18})) of certain excited states of Er^{3+} doped different chlorophosphate glasses

Transition		LiCPG		NaCPG		KCPG		CaCPG		PbCPG	
		β	Σ	β	Σ	β	Σ	β	Σ	β	Σ
$^4G_{11/2}\rightarrow$	$^2H_{9/2}$	0	0.30	0	0.17	0	0.52	0	0.81	0	0.88
	$^4F_{3/2}$	0	0.04	0	0.05	0	0.06	0	0.09	0	0.11
	$^4F_{5/2}$	0	0.05	0	0.05	0	0.06	0	0.10	0	0.12
	$^4F_{7/2}$	0	0.25	0	0.14	0	0.30	0	0.56	0	0.80
	$^2H_{11/2}$	0	0.14	0	0.15	0	0.07	0	0.21	0	0.45
	$^4S_{3/2}$	0	0.11	0	0.11	0	0.01	0	0.12	0	0.36
	$^4F_{9/2}$	0.03	1.58	0.01	0.58	0.03	2.63	0.03	4.25	0.04	5.06
	$^4I_{9/2}$	0.01	0.33	0	0.14	0.01	0.54	0.01	0.87	0.01	1.02
	$^4I_{11/2}$	0	0.10	0	0.10	0	0.04	0	0.14	0	0.31
	$^4I_{13/2}$	0.1	1.64	0.09	1.26	0.07	2.01	0.09	3.55	0.11	4.79
	$^4I_{15/2}$	0.84	7.62	0.87	6.66	0.87	12.59	0.85	18.49	0.82	19.77
$^4F_{5/2}\rightarrow$	$^4F_{7/2}$	0	0.12	0	0.06	0	0.19	0	0.30	0	0.36
	$^2H_{11/2}$	0	0.13	0	0.13	0	0.19	0	0.29	0	0.32
	$^4S_{3/2}$	0	0.02	0	0	0	0.03	0	0.05	0	0.06
	$^4F_{9/2}$	0.04	0.76	0	0.77	0.02	0.89	0.03	1.49	0.04	2.02
	$^4I_{9/2}$	0.04	0.38	0.03	0.35	0.03	0.52	0.04	0.83	0.05	1.06
	$^4I_{11/2}$	0.03	0.24	0.03	0.23	0	0.03	0.02	0.27	0.05	0.79
	$^4I_{13/2}$	0.41	1.54	0.40	1.59	0.32	1.96	0.36	3.14	0.43	3.93
	$^4I_{15/2}$	0.47	0.89	0.49	0.97	0.60	1.78	0.54	2.32	0.43	1.92
$^4F_{7/2}\rightarrow$	$^2H_{11/2}$	0	0.14	0	0.11	0	0.27	0	0.39	0	0.41
	$^4S_{3/2}$	0	0	0	0.01	0	0	0	0	0	0
	$^4F_{9/2}$	0	0.06	0	0.04	0	0.07	0	0.13	0	0.20
	$^4I_{9/2}$	0.04	0.66	0.03	0.65	0.04	1.08	0.04	1.55	0.03	1.62
	$^4I_{11/2}$	0.05	0.64	0.05	0.64	0.03	0.47	0.04	1.06	0.06	1.88
	$^4I_{13/2}$	0.12	0.71	0.11	0.70	0	0.04	0.06	0.79	0.15	2.34
	$^4I_{15/2}$	0.78	2.22	0.80	2.36	0.92	3.54	0.85	5.07	0.74	5.31
$^4S_{3/2}\rightarrow$	$^4F_{9/2}$	0	0.02	0	0.02	0	0.04	0	0.05	0	0.04
	$^4I_{9/2}$	0.04	0.56	0.03	0.59	0.02	0.86	0.03	1.27	0.04	1.39
	$^4I_{11/2}$	0.02	0.18	0.02	0.19	0.01	0.33	0.02	0.46	0.02	0.40
	$^4I_{13/2}$	0.27	1.11	0.27	1.19	0.26	2.16	0.27	2.88	0.27	2.39
	$^4I_{15/2}$	0.66	1.11	0.67	1.21	0.68	2.22	0.67	2.90	0.66	2.43
$^4F_{9/2}\rightarrow$	$^4I_{9/2}$	0.01	0.14	0	0.05	0.02	0.24	0.01	0.38	0.01	0.46
	$^4I_{11/2}$	0.02	0.13	0.02	0.13	0.03	0.17	0.03	0.27	0.02	0.32
	$^4I_{13/2}$	0.41	0.69	0.43	0.75	0.86	1.33	0.58	1.76	0.31	1.49
	$^4I_{15/2}$	0.55	0.30	0.54	0.30	0.55	0.04	0.36	1.40	0.65	0.98
$^4I_{9/2}\rightarrow$	$^4I_{11/2}$	0	0.05	0	0.05	0	0.06	0	0.11	0	0.13
	$^4I_{13/2}$	0.29	0.46	0.31	0.50	0.83	0.87	0.46	1.16	0.21	0.98
	$^4I_{15/2}$	0.70	0.24	0.68	0.24	0.68	0.69	0.53	0.29	0.78	0.79
$^4I_{11/2}\rightarrow$	$^4I_{13/2}$	0.12	0.47	0.13	0.48	0.10	0.80	0.11	1.13	0.11	1.12
	$^4I_{15/2}$	0.88	0.46	0.87	0.43	0.89	0.89	0.89	1.20	0.88	1.08
$^4I_{13/2}\rightarrow$	$^4I_{15/2}$	1.00	0.83	1.00	0.87	1.00	1.56	1.00	2.07	1.00	1.93

chlorophosphate glass than in different chloroborate [22], fluorophosphate [16] and aluminium phosphate [23] glasses. Hence there is a strong ionic nature of the metal ligand bond in sodium chlorophosphate glasses and low asymmetry of the local environment. Nageno et al. [35] shown that Ω_4 and Ω_6 parameters of silicate and borate glasses (but not of phosphate glasses) increase with increasing of ion packing ratios (V_P) of the glass host. In the present work also we have not

observed any relation between ion packing ratios and intensity parameters.

4.5. Radiative lifetimes and branching ratios

Using the expressions given in theoretical part, electric dipole line strengths (S_{ed}), radiative transition probabilities (A), branching ratios (β) and integrated cross sections (Σ) for stimulated emission for certain excited states $^4G_{11/2}$, $^4F_{5/2}$, $^4F_{7/2}$, $^4S_{3/2}$, $^4F_{9/2}$, $^4I_{9/2}$, $^4I_{11/2}$ and $^4I_{13/2}$ of Er^{3+} doped chlorophosphate glasses have been calculated. These results are presented in Table 6 for lithium chlorophosphate glass. The calculated branching ratios (β) of certain transitions of Er^{3+} ion in lithium chlorophosphate glass are compared with zinc chloride [15] and zinc borate glasses [36] in the same table. Takebe et al. [23] observed the relationship between spontaneous emission probabilities and the ion packing ratios for Er^{3+} doped oxide glasses. According to that, emission probabilities increase with increasing ion packing ratios only in silicate and oxide glasses but not in phosphate glasses. In the present work, we also have not observed any relation between ion packing ratios and emission probabilities. Estimated radiative lifetimes (τ_R) for all the above excited states are portrayed in Table 7 along with the lifetimes estimated in other glass matrices. The radiative lifetimes of the excited states $^4F_{5/2}$, $^4F_{7/2}$, $^4S_{3/2}$ and $^4I_{13/2}$ are decreasing with the substitution of lithium, sodium, potassium, calcium and lead chlorides in the above glass matrix. For the remaining excited states also, the lifetimes are in decreasing trend (except $^4G_{11/2}$ of sodium glass and $^4F_{9/2}$ and $^4I_{9/2}$ of potassium glass) with the above various environments. It is observed that the magnitudes of lifetimes are slightly higher in the case of chlorophosphate glasses than in fluoride and zinc borate glasses. The lifetime of $^4I_{9/2}$ in potassium chlorophosphate glass is very high. It may be due to the smaller value of Ω_4 parameter which is observed in this glass.

Table 8 gives the comparison of branching ratios (β) and integrated cross sections (Σ) for all the transitions of Er^{3+} ion in all the chlorophosphate glasses. It is observed from the table that the branching ratios and integrated cross sections of the transitions $^4F_{5/2} \rightarrow {}^4F_{15/2}$, $^4F_{7/2} \rightarrow {}^4I_{15/2}$ and $^4S_{3/2} \rightarrow {}^4I_{15/2}$ are increasing with lithium, sodium

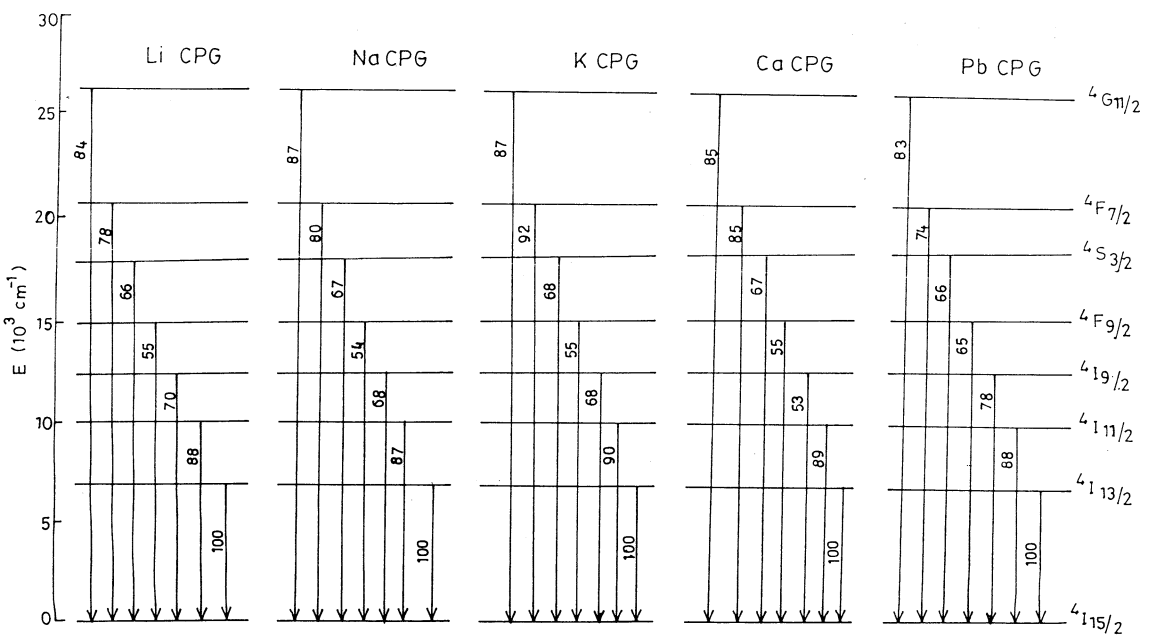

Fig. 6. Energy level diagrams for luminescent transitions of Er^{3+} ion in chlorophosphate glasses.

and potassium and further decreasing to calcium and lead glasses. In the case of $^4G_{11/2} \rightarrow {}^4I_{15/2}$, $^4F_{9/2} \rightarrow {}^4I_{15/2}$ and $^4I_{I9/2} \rightarrow {}^4I_{15/2}$ transitions, the branching ratios are more or less the same for the above three glasses. Some of the potential lasing transitions are identified from the magnitudes of their branching ratios and are depicted in Fig. 6. From the above studies, it is concluded that lithium and potassium chlorophosphate glasses doped with Er^{3+} ion are useful for laser excitation.

5. Conclusions

Though the optical band gaps (E_{opt}) are not particularly sensitive to diferent types of chlorides in the glass compostion, the optical band gaps decrease with the increase of average molecular weight of the glass for only alkali elements (Li, NA and K) for both direct and indirect transitions. The largest optical band gaps have been recorded in the case of sodium and calcium glasses for direct and indirect transitions, respectively. With regard to the physical properities, the ion packing ratio decreases with the decrease of ionic radius in the order Ca > K > Li > Pb > Na. Among all the glasses studied, sodium chlorophosphate glass shows peculiar physical properties.

The cut off region starts from 400 nm only in sodium chlorophosphate glass among all the Er^{3+} doped glasses. The spectral intensities of the transitions of Er^{3+} are very high in lead chlorophosphate glass among all the glasses studied. The intensities of the hypersensitive transitions decreased with the decrease of Ω_2 parameter which is in accordance with the theory. Ω_4 parameter decreased and Ω_6 parameter increased with the increase of average molecular weight of the glass only for alkali elements (Li, Na and K). There has not been any relation observed between ion packing ratios and emission probabilities. The estimated radiative lifetimes are more or less similar for certain excited states of Er^{3+} in different chlorophosphate glasses. From the branching ratios and integrated absorption cross sections, it can be concluded that the transitions $^4I_{11/2} \rightarrow {}^4I_{15/2}$ and $^4F_{9/2} \rightarrow {}^4I_{15/2}$ are more powerful for lasting action in these chlorophosphate glasses.

Acknowledgements

The authors are grateful to Prof. V. Padmanabha Sarma, Department of Physics, for providing the necessary facilities. One of the authors Dr RPSC, is highly thankful to the Council of Scientific and Industrial Research, New Delhi, for the award of a Research Associate Fellowship.

References

[1] M.J. Weber, K.A. Saroyan, R.C. Ropp, J. Non-Cryst. Solids 44 (1981) 137.
[2] M.J. Weber, K.A. Saroyan, R.C. Ropp, J. Non-Cryst. Solids 74 (1985) 167.
[3] J. Yasi, J. Shibin, J. Yanyan, J. Non-Cryst. Solids 112 (1989) 286.
[4] H. Ebendorf-Heidepriem, W. Seeber, D. Ehrt, Phys. Stat. Solid. A 157 (1990) 723.
[5] V.P. Gapontsev, S.M. Matitsin, A.A. Isineev, V.B. Kravchenko, Optics Laser Technol. 14 (1982) 189.
[6] Selected papers on Rare-earth doped fiber laser sources and amplifiers, SPIE Milestone series volume MS 37, ed. M.J.F. Digonnet (1992).
[7] R.I. Mears, L. Reekie, I.M. Jauncey, D.N. Payne, Electron. Lett. 23 (1987) 1026.
[8] T. Kitagawa, K. Hattori, K. Shuto, M. Yasu, M. Kobayashi, M. Horiguchi, Electron. Lett. 28 (1992) 1818.
[9] E. Snitzer, R. Woodcock, Appl. Phys. Lett. 6 (1965) 45.
[10] J.Q. Edwards, J.N. Sandoe, J. Phys. D 7 (1974) 107.
[11] E. Snitzer, R. Woodcock, J. Sergre, IEEE J. Quantum Electr. QE-4 (1968) 360.
[12] Shibin Jiang, Michael Myers, Nasser Reyghambarian, J. Non-Cryst. Solids 239 (1998) 143.
[13] H. Higuchi, M. Takahashi, Y. Kawamoto, J. Appl. Phys. 83 (1998) 19.
[14] D.A. Turnbull, B.G. Aitken, S.G. Bishop, J. Non-Cryst. Solids 244 (1999) 260.
[15] M. Shojiya, M. Takahashi, R. Kanno, Y. Kawamoto, K. Kadono, J. Appl. Phys. 82 (1997) 6259.
[16] K. Binnemans, R. VanDeun, C. Gorller-Walrand, J.L. Adam, J. Non-Cryst. Solids 238 (1998) 11.
[17] R. Van Deun, K. Binnemans, C. Gorller-Walrand, J.L. Adam, J. Alloys Compounds 283 (1999) 59.
[18] S. Tanabe, N. Sugimoto, S. Ito, T. Hanada, J. Lumin. 87-89 (2000) 670.
[19] Xian Feng, S. Tanabe, T. Hanada, J. Appl. Phys. 89 (2001) 3560.

[20] Xian Feng, S. Tanabe, T. Hanada, J. Am. Ceram. Soc. 84 (2001) 165.
[21] S.V.J. Lakshman, Y.C. Ratnakaram, Phys. Chem. Glasses 31 (1989) 42.
[22] Y.C. Ratnakaram, N. Sudharani, J. Non-Cryst. Solids 217 (1997) 291.
[23] H. Takebe, K. Morinaga, T. Izumitani, J. Non-Cryst. Solids 178 (1994) 58.
[24] M.M. Ahmad, C.A. Hogarth, M.N. Khan, J. Mater. Sci. Lett. 19 (1984) 4040.
[25] R. Harinath, S. Buddudu, F.J. Bryant, Solid State. Comm. 749 (1990) 1147.
[26] F.A. Davis, N.F. Mott, Phil. Mag. 22 (1970) 903.
[27] E.Y. Wong, J. Chem. Phys. 35 (1961) 544.
[28] E.Y. Wong, J. Chem. Phys. 38 (1963) 976.
[29] B.R. Judd, Phys. Rev. 127 (1962) 750.
[30] G.S. Ofelt, J. Chem. Phys. 37 (1962) 511.
[31] W.T. Carnall, H. Cross White, H.M. Cross White. Energy level structure and transition probabilities of the trivalent lanthanides in LaF_3, Argonne National Laboratory Report, ANL-7-XX, (1978).
[32] K. Morinaga, T. Ito, Y. Suginohara, T. Yanagase, J. Jpn. Inst. Met. 38 (1974) 1065.
[33] R.D. Peacock, Structure and Bonding, vol. 22, Springer, Berlin, 1975, p. 83.
[34] C.K. Jorgensen, R. Reisfeld, J. Less Comm. Met. 93 (1983) 107.
[35] Y. Nageno, H. Takebe, K. Morinaga, J. Am. Ceram. Soc. 76 (1993) 3081.
[36] G. Pozza, D. Ajo, M. Bettinelli, A. Speghini, M. Casarin, Solid State Comm. 97 (1996) 521.
[37] D.C. Yeh, R.R. Petrin, W.A. Sibly, V. Madigou, J.L. Adam, M.J. Suscavage, Phys. Rev. B 39 (1989) 80.